

# Evaluation of the electromechanical behavior of polyvinylidene fluoride used as a component of risers in the offshore oil industry

Khrissy Aracélly Reis Medeiros<sup>1,\*</sup>, Eduardo Queirós Rangel<sup>2</sup>, Alexandre Ribeiro Sant'Anna<sup>2</sup>, Daniel Ramos Louzada<sup>3</sup>, Carlos Roberto Hall Barbosa<sup>3</sup>, and José Roberto Moraes d'Almeida<sup>1</sup>

<sup>1</sup> Department of Chemical Engineering and Materials, Catholic University of Rio de Janeiro, Rio de Janeiro, RJ, Brazil

<sup>2</sup> Department of Mechanical Engineering, Catholic University of Rio de Janeiro, Rio de Janeiro, RJ, Brazil

<sup>3</sup> Postgraduate Metrology Programme, Catholic University of Rio de Janeiro, Rio de Janeiro, RJ, Brazil

Received: 18 January 2018 / Accepted: 29 August 2018

**Abstract.** A sample of polyvinylidene fluoride removed from a riser component was tested in laboratory to evaluate its electromechanical behavior. For this, an experimental setup was developed, after Fourier Transform Infrared Spectroscopy (FTIR) results have shown through the absorption bands, that this sample had a spectrum of the piezoelectric phase  $\beta$ . In order to identify if such sample would be able to respond electrically to the application of external mechanical excitation applied by a shaker, measurements were made of the induced voltages by piezoelectric effect, with varying accelerations and frequencies. The results indicated that the material, although it has not been processed for this purpose, responds electrically to the applied mechanical stimulus, demonstrating a good correlation between the measured signals and the accelerations.

## 1 Introduction

The poly (vinylidene fluoride) – PVDF is a thermoplastic polymer that presents important properties that qualify it for different applications, such as: sensors, robotics, security elements, acoustic and optical devices, mechanical accessories, automotive and traffic devices, sports and leisure goods [1]. It is also applied in fluid handling, in hot water piping systems, in ultra-pure water systems for the semiconductor industry, in packaging and in chemical plants [2], among others.

Despite its attractive specific mechanical properties [3], it is its piezoelectric property that motivates most of the works, since the piezoelectricity occurs in few materials and is more intense in PVDF relative to other polymers.

Poly (vinylidene fluoride) is a semicrystalline polymer containing one or more crystalline phases, known as  $\alpha$ ,  $\beta$ ,  $\gamma$  and  $\delta$ , dispersed in the amorphous regions [4]. These phases can be interconverted by the application of mechanical, thermal or electrical energy [5]. The PVDF piezoelectricity phenomenon comes from the dipoles created by the atoms of positive hydrogen and the negative fluorine, which are entirely aligned in the structure of the main chain ( $-\text{CF}_2-\text{CH}_2-$ ) of planar conformation of the  $\beta$ -phase. This structure (Fig. 1) shows the dipoles arranged in parallel, and the whole main chain is perpendicular to the direction

of the dipoles, thus generating a strong polarization that results in the piezoelectric behavior of the material [6–9].

The electroactive phase  $\beta$  gives to the polymer characteristics of an electroelastic material that exhibits electromechanical coupling. That is, it experiences mechanical deformations when placed in an electric field, and becomes electrically polarized under mechanical loads [10].

Due to the mechanical and chemical stability of PVDF [11], a common industrial application of this material is in the layers that make up risers used in the oil industry, acting as an effective barrier to most fluids and gases transported in the exploration and production of oil and natural gas, even at elevated temperatures [12].

The use of PVDF in deep sea systems, as well as all failure modes that may occur under service conditions, are not yet well detailed in the literature. In this context, it is important to consider that little has been discussed about the influence the processing of the polymer on its barrier properties [13].

Typically, for this application, is not expected that the PVDF presents the piezoelectric phase- $\beta$ . However, during the processing by extrusion occurs a mechanical elongation of material, where the PVDF is forced in the longitudinal direction (towards the axis of the tube) and there may be a phase transformation  $\alpha \rightarrow \beta$ .

In this sense, the aim of this work is to investigate if a non-polarized sample removed from a commercial grade of extruded PVDF, which presents the electroactive  $\beta$  phase is able to generate electrical voltages due to the

\* Corresponding author: [khrissymedeiros@gmail.com](mailto:khrissymedeiros@gmail.com)

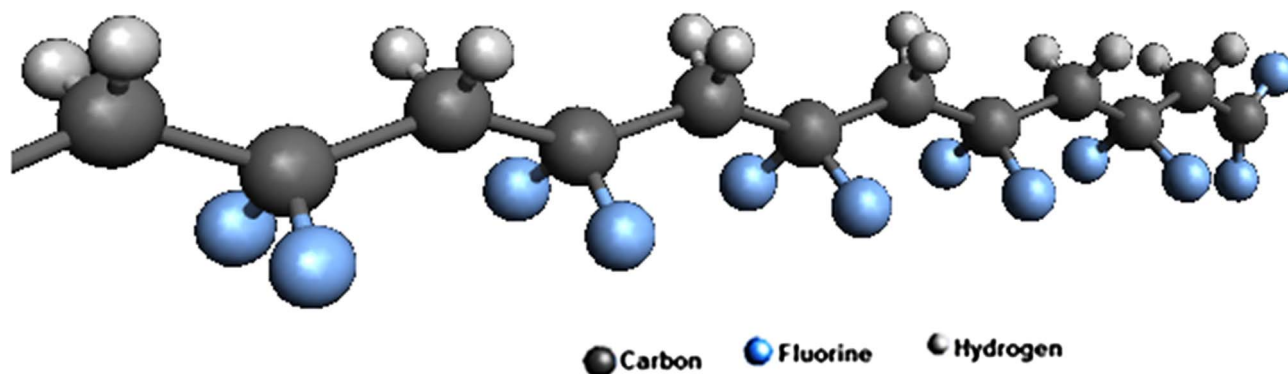


Fig. 1. PVDF- $\beta$  planar conformational structure.



Fig. 2. Extruded PVDF from where the sample was removed.

piezoelectric phenomenon induced only by the effect of material processing.

## 2 Materials and methods

### 2.1 Non-polarized extruded sample

A non-polarized sample was removed from an extruded PVDF grade (Fig. 2) manufactured to operate as a pressure barrier or sealing layer on flexible multilayer lines (risers) in the oil industry.

This PVDF pressure barrier is manufactured by continuous extrusion of polymer onto a metallic carcass (Fig. 3). The extrusion molding basically consists of a process where a mechanical screw propels through a chamber the



Fig. 3. External representation of the flexible tube – riser.

pelletized material, which is successively compacted, melted, and formed into a continuous stream of viscous fluid. Extrusion takes place as this molten mass is forced through a die orifice. Solidification of the extruded length is expedited by blowers, a water spray or bath some time before passing by a moving conveyor. The technique is especially adapted to producing continuous lengths having constant cross-sectional geometries. The carcass is a corrugated metal tube with a specific internal diameter, supporting the extruded barrier and preventing its collapse by pressure or crushing due to the loads applied during pipe operation [14, 15].

The extracted sample was characterized by means of Fourier Transform Infrared Spectroscopy (FTIR) using the Attenuated Total Reflectance (ATR) technique. A

Speckin 400 spectrophotometer with diamond crystal was used, operating in the region of  $4500\text{--}650\text{ cm}^{-1}$  (medium field) with a resolution of  $4\text{ cm}^{-1}$  and 16 scans.

The FTIR spectra of PVDF provides valuable information about its structure, allowing to distinguish between the different crystalline forms [16] that have been extensively investigated and are widely documented in the literature [16–28].

In Figure 4, it is shown the FTIR spectrum corresponding to the non-polarized sample removed from an extruded PVDF grade, where the predominant presence of the beta electroactive phase can be clearly observed, as valleys in the spectrum that indicate absorption of some specific wavenumbers (or bands). Table 1 presents the references that associate the observed bands with each phase of the polymer.

Due to the identification of the presence of  $\beta$  phase in the sample by FTIR, an experiment in laboratory was developed to verify if this sample was able to respond electrically to the external mechanical excitation and to know the signal intensity, resonance frequencies and other variables involved.

With this purpose, the sample is submitted to the application of external excitations. The tests were performed to identify the stress levels generated from the use of controlled mechanical stimuli. On account of PVDF being a dielectric material, it is necessary to install electrodes in the sample, for the measurement of the voltage eventually induced by the piezoelectric mechanism. Moreover, a variation in the positioning of the electrodes in the sample was adopted in order to evaluate the influence of this parameter on the behavior of the signal.

### 3 Experimental setup

The experimental setup (Fig. 5) used to test the sample consists of the Brüel & Kjær Charge Amplifier (Type 2719), National Instruments digitizer device (NI USB-6229) and also the following elements:

1. Sample PVDF ( $20.0\text{ cm} \times 2.5\text{ cm}$ );
2. Permanent Magnet Vibration Exciter (Type 4808) – shaker;
3. Two Brüel & Kjær accelerometers (Type 4513);
4. Electrodes – copper tape with conductive adhesive; and
5. Support base.

The experiment was configured with the mechanical shaker equipped with a specially designed support for stable and reproducible fixation of the sample.

For control of measuring equipment, signal processing and recording of experimental data, routines have been developed in LabVIEW™.

Figure 5a presents two electrodes positioned in a configuration in which these electrodes are outside of the support base. On the other hand, in Figure 5b, one of the electrodes is positioned inside this support base, where the sample is crimped.

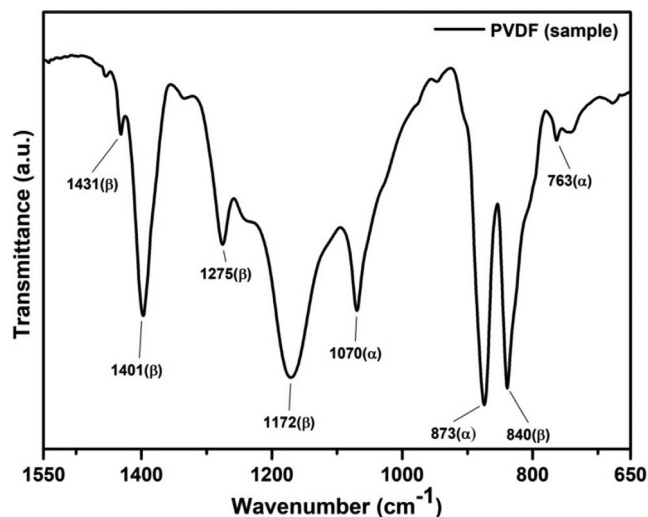


Fig. 4. FTIR transmission spectra of PVDF sample.

Table 1. Absorption FTIR bands characteristics of  $\alpha$  and  $\beta$ -PVDF.

Band ( $\text{cm}^{-1}$ )	Phase	References
763	$\alpha$	[25, 26, 28]
873		[23]
1070		[20]
840	$\beta$	[16–18, 20–22, 24–27]
1172		[20]
1275		[27, 28]
1401		[24]
1431		[19]

These configurations with different positioning were used to verify how this positioning affects the signal. That is, to check whether the positioning of the electrodes inside the support base and outside it influences the signal intensity.

### 4 Tests performed

Initially, spectral measurements were performed in order to identify the main resonant frequencies of the assembly and the PVDF signal. The two commercial accelerometers, with  $10\text{ mV/g}$  nominal sensitivities (“g” being the acceleration of gravity), were used as reference standards for these measurements.

The electrical signals measurements, obtained by the piezoelectric effect in the sample, were performed using a 16-bit acquisition system (NI-USB 6229) with a fixed sampling frequency of  $25\,600\text{ Hz}$ .

Initially, resonant frequencies of the structure were identified by frequency domain analysis (spectral analysis) with white noise excitation. This analysis was performed in two

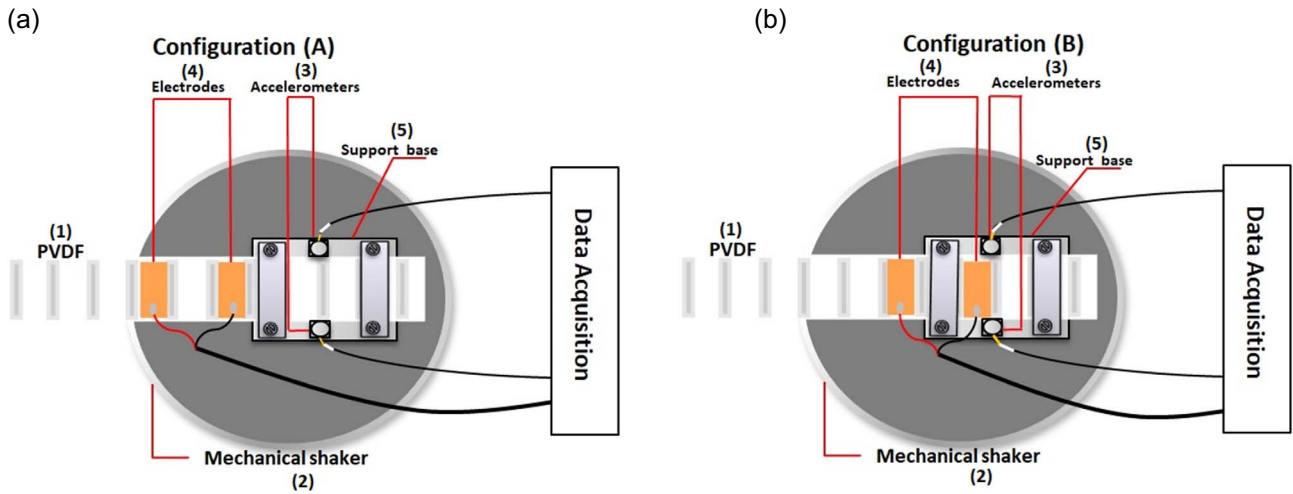


Fig. 5. Schematics of the setup: (a) Configuration A; (b) Configuration B.

stages, with the first stage covering a frequency range from 10 Hz to 810 Hz, and the second stage in the range from 810 Hz to 8400 Hz. This division in stages allows for better resolution in frequency, mainly in the lower range.

After these initial tests, the procedure for characterization of the sample piezoelectric behavior consisted on the measurement of the electrical signal measured in the sample, with the level of vibration (expressed in units of *g*, the acceleration of gravity) kept constant, taking as a reference the average between the two signals of the reference accelerometers. The excitation signal was sinusoidal with discretely scanned frequencies as follows:

- 1 Hz steps for frequencies between 10 Hz and 100 Hz;
- 10 Hz steps for frequencies between 100 Hz and 1000 Hz; and
- 50 Hz steps for frequencies between 1000 Hz and 8000 Hz.

This procedure was performed for 1*g*, 2*g* and 3*g* vibration levels and was performed for the two electrode positioning configurations shown in Figure 5.

## 5 Results

### 5.1 White noise analysis

The results were combined in a single graph, shown in Figure 6. From this measurement some points of interest were identified, with the most significant resonance being around 55 Hz. It was also identified electromagnetic interference from the electric network at 60 Hz and harmonics.

This white noise analysis allows the structure to be excited at all frequencies at the same time so that if there are interferences (constructive or destructive) they will be more easily identified. In addition, such test is more practical since it is not necessary to evaluate frequency by frequency.

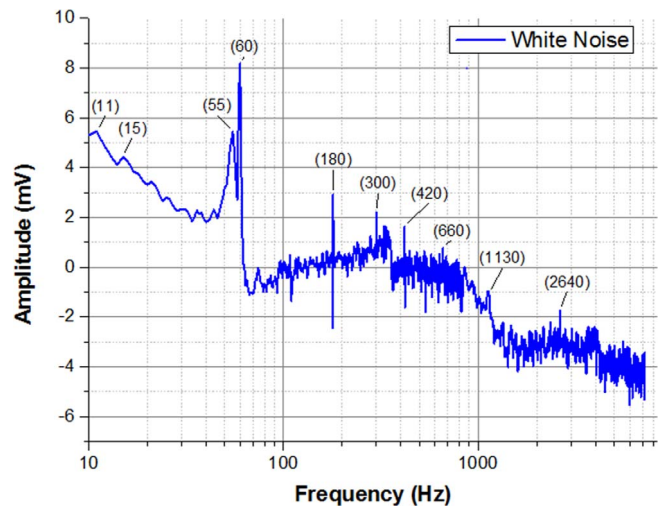


Fig. 6. Resonant frequencies of the experimental assembly for white noise excitation.

### 5.2 Piezoelectric behavior of the PVDF sample

Figure 7 refers to the two electrode positioning configurations adopted to test the sample shown in Figure 5 using the frequency sweep described in Section 3. The results of the amplitude of the output signal of PVDF relating to the configuration A are shown in Figure 7a, while the results obtained according to the configuration B can be seen in Figure 7b.

The aim of using two different configurations, rather than one, is to verify exactly if this influences in some way the results. Note that the resonant frequency of the assembly is clearly located at 55 Hz and also it was found that for the two positioning configurations of the electrodes shown in Figure 5, the amplitude of the signal measured in the sample increases with increasing acceleration. However, for the positioning described in Figure 5b, the amplitudes are larger. When observing the range corresponding to

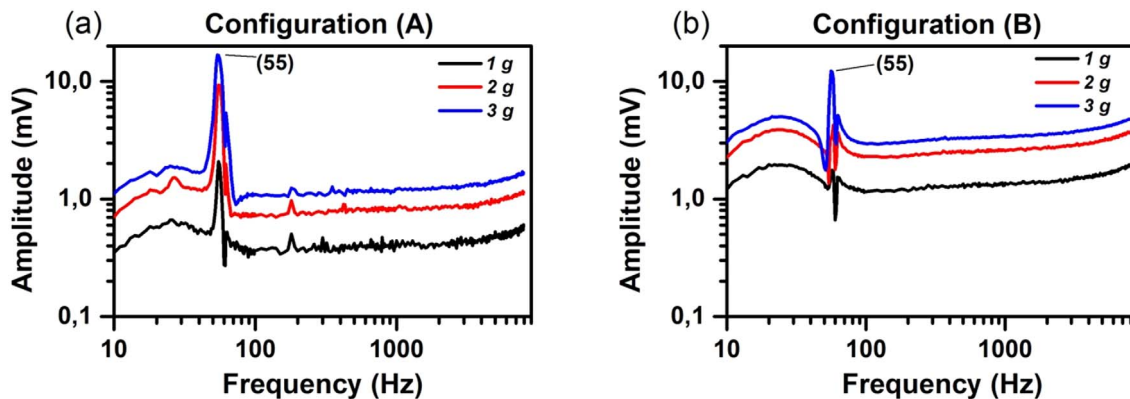


Fig. 7. Typical PVDF signal: (a) Configuration A; (b) Configuration B.

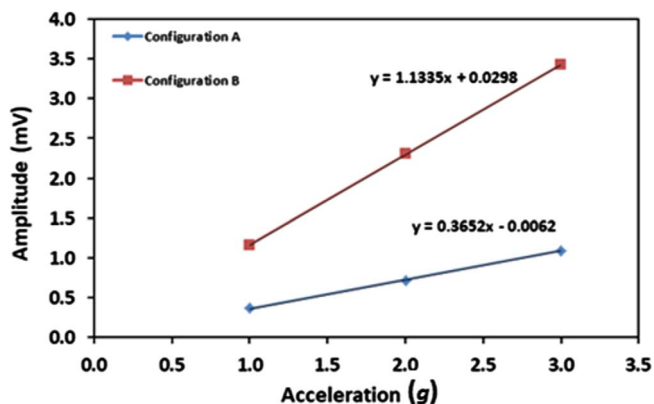


Fig. 8. Estimated sensitivities to 100 Hz.

the linear region in Figure 7b, the amplitude values are between 0 mV and 1.5 mV, while in Figure 7a these values are between 1.0 mV and 3.5 mV.

This can also be seen in Figure 8, which shows for each level of vibration the corresponding amplitudes referring to 100 Hz.

These results allowed estimating the PVDF sensitivity values for each of the electrode configurations. With this, the frequency of 100 Hz was considered and from the amplitude data of all vibration levels tested (1g, 2g and 3g) the sensitivities were estimated for the two configurations.

The estimated sensitivity for Figure 5a configuration is 0.36 mV/g and for Figure 5b configuration is 1.13 mV/g.

## 6 Discussion

In this study a non-polarized sample was obtained from an extruded PVDF grade (Fig. 2). The crystalline phases present in sample were confirmed by FTIR.

However, when one tries to analyze the spectrum of a given PVDF sample on the basis of the results of previous vibrational spectra, some problems may be encountered mainly because a large number of publications show discordant results.

This is due to the fact that each PVDF sample has been generally obtained from different materials (molecular mass and distribution, head-to-head and tail-to-tail defects, crystalline nature, orientation) or by different experimental conditions (sample type, instrument, etc.) [16, 20].

In addition, some bands of FTIR spectra of PVDF are simultaneously common to the  $\beta$  and  $\gamma$ -phases, such as 811  $\text{cm}^{-1}$ , 839  $\text{cm}^{-1}$  [20], 840  $\text{cm}^{-1}$  [16, 19, 29] and 1234  $\text{cm}^{-1}$  [28]; others are easily attributed to polymer chain defects (678, 1330, 1450  $\text{cm}^{-1}$ ) [20]; and some are associated to the amorphous phase of the polymer, such as 488  $\text{cm}^{-1}$ , 600  $\text{cm}^{-1}$ , 880  $\text{cm}^{-1}$  [21], 890  $\text{cm}^{-1}$  [19], 497  $\text{cm}^{-1}$ , 517  $\text{cm}^{-1}$ , 904  $\text{cm}^{-1}$ , 1194  $\text{cm}^{-1}$  and 1247  $\text{cm}^{-1}$  [25].

Indeed, the characteristic bands of  $\beta$ - and  $\gamma$ -phases in the range from 833  $\text{cm}^{-1}$  to 840  $\text{cm}^{-1}$  [26] and from 508  $\text{cm}^{-1}$  to 512  $\text{cm}^{-1}$  [16] are very close in the FTIR spectra and are often difficult to distinguish. On the other hand, the bands around at 763  $\text{cm}^{-1}$  and/or 614  $\text{cm}^{-1}$ , 1275  $\text{cm}^{-1}$  and 1234  $\text{cm}^{-1}$  can be consistently used to differentiate and identify the  $\alpha$ ,  $\beta$  and  $\gamma$  phases, respectively [18].

Particularly, in the case of the 840  $\text{cm}^{-1}$  band, for instance, that some authors [13–15, 17–19, 21–24] classify as a  $\beta$ -phase characteristic, while others [16, 29, 30] consider common to both phases ( $\beta$  and  $\gamma$ ), it has been recently accepted [16] that the band at 840  $\text{cm}^{-1}$  is common to both polymorphs but it is a strong band just for the  $\beta$ -phase, whereas for the  $\gamma$ -phase it appears as a shoulder of the 833  $\text{cm}^{-1}$  band, which is characteristic of  $\gamma$ -PVDF.

Therefore, in the FTIR spectra corresponding to Figure 4, the absorption band observed at 840  $\text{cm}^{-1}$  can be assigned just to  $\beta$ -phase.

It is known that the primary reason for the piezoelectricity in PVDF is related to the crystal structure of this polymer, in particular with the  $\beta$ -phase [26]. In view of the presence of phase- $\beta$  in said sample, the procedure presented in Figure 5, in which the sample was submitted to the application of external excitations, was carried out to test its electrical behavior, as it is would be made with any other material notoriously piezoelectric.

In the results it was observed that the signal-to-noise ratio improves with increasing acceleration, as expected.

In addition, it was also demonstrated that the output signal of PVDF is larger for the positioning described in

Figure 5b, namely, for the B configuration. In this configuration, one of the electrodes is closest to the base and the other is on the base, this means a larger deformation compared to configuration A.

## 7 Conclusion

This work demonstrated that the extruded PVDF sample, without any treatment, as the polarization required for the alignment of the dipoles within the sample, for example, is able to generate voltage only by the effect of the processing (from extrusion) which in itself induces the formation of the piezoelectric phase  $\beta$ . And even though there are no potential applications today, this behavior may prove to be useful at some point for future electromechanical applications.

In the scope application of PVDF in risers, the frequencies tested in the laboratory are superior to those to which the risers are typically submitted [31]. In addition, the voltage levels generated in the experimental conditions are very small, but were measured in a small sample (20.0 cm  $\times$  2.5 cm). However, it is known (by piezoelectric constitutive law) that the voltage is directly proportional to the thickness of the material, this means, the more material, the higher is the electrical voltage generated [32].

Therefore, although it is not possible to specify the risks involved, it is important to ensure that the piezoelectric behavior of the PVDF does not introduce mechanisms of electrical failure in the material.

In addition, the identification of unintentional piezoelectric behavior in a non-polarized sample removed from a commercial grade of extruded PVDF suggests that for the effect of this application the influence of the polymer processing and the piezoelectric phenomenon should be carefully considered.

*Acknowledgments.* The authors thank for the financial support provided by The Brazilian National Council for Scientific and Technological Development (CNPq: Conselho Nacional de Desenvolvimento Científico e Tecnológico), Studies and Projects Foundation (FINEP: Financiadora de Estudos e Projetos) and Research Support Foundation of the State of Rio de Janeiro (FAPERJ: Fundação de Amparo à Pesquisa do Estado do Rio de Janeiro).

## References

- Vijayakumar R.P., Khakhar D.V., Misra A. (2010) Studies on  $\alpha$  to  $\beta$  phase transformations in mechanically deformed PVDF films, *J. Appl. Polym. Sci.* **117**, 6.
- Brydson J.A. (1995) *Plastics materials*, Butterworth-Heinemann Ltd., Oxford.
- Le Gac P.-Y., Davies P., Choqueuse D. (2015) Evaluation of long term behaviour of polymers for offshore oil and gas applications, *Oil Gas Sci. Technol. - Rev. IFP Energies nouvelles* **70**, 2, 279–289.
- Harrison J.S., Ounaies Z. (2001) *Piezoelectric Polymers*, NASA Technical Reports Server (NTRS), Hampton, Virginia, EUA.
- Gregorio R., Borges D.S. (2008) Effect of crystallization rate on the formation of the polymorphs of solution cast poly(vinylidene fluoride), *Polym.* **49**, 18, 4009–4016.
- Ueberschlag P. (2001) PVDF piezoelectric polymer. *Sens. Rev.* **21**, 2, 118–126.
- Zhu G.D., Zeng Z.G., Zhang L., Yan X.J. (2008) Piezoelectricity in  $\beta$ -phase PVDF crystals: A molecular simulation study, *Comput. Mater. Sci.* **44**, 2, 224–229.
- Poulsen M., Ducharme S. (2010) Why ferroelectric polyvinylidene fluoride is special, *IEEE Trans. Dielectr. Electr. Insul.* **17**, 4, 1028–1035.
- Li L., Zhang M., Rong M., Ruan W. (2014) Studies on the transformation process of PVDF from  $\alpha$  to  $\beta$  phase by stretching, *RSC Adv.* **4**, 8, 3938–3943.
- Yang J. (2005) *An introduction to the theory of piezoelectricity*, Springer Science + Business Media, Inc., Nebraska-Lincoln, USA.
- Lefebvre X., Pasquier D., Gonzalez S., Epsztein T., Chirat M., Demanze F. (2015) Development of reactive barrier polymers against corrosion for the oil and gas industry: From formulation to qualification through the development of predictive multiphysics modeling, *Oil Gas Sci. Technol. - Rev. IFP Energies nouvelles* **70**, 2, 293–303.
- Marion A., Rigaud J., Werth M., Martin J. (2002)  $\gamma$ -Flex: A new material for high temperature flexible pipes, *Proceedings of Offshore Technology Conference, OTC, Onepetro, May Houston, Texas*, MS-14327, 6–9.
- Klopffer M.H., Berne P., Espuche E. (2015) Development of innovating materials for distributing mixtures of hydrogen and natural gas. Study of the barrier properties and durability of polymer pipes, *Oil Gas Sci. Technol. - Rev. IFP Energies nouvelles* **70**, 2, 305–315.
- Callister W.D., Rethwisch D.G. (2009) *Materials science and engineering: An introduction*, John Wiley & Sons.
- Fernando U.S., Davidson M (2015) Fatigue Life Assessment of Single Layer 60512 PVDF Barrier in Unbonded Flexible Risers. *ASME 34th International Conference on Ocean, Offshore and Arctic Engineering, Volume 5B: Pipeline and Riser Technology St. John's, Newfoundland, Canada, May 31–June 5*
- Martins P., Lopes A.C., Lanceros-Mendez S. (2014) Electroactive phases of poly(vinylidene fluoride): Determination, processing and applications, *Prog. Polym. Sci.* **39**, 4, 683–706.
- Costa L.M.M., Bretas R.E.S., Filho G.R. (2009) Caracterização de filmes de PVDF- $\beta$  obtidos por diferentes técnicas, *Polím* **19**, 3, 183–189.
- Salimi A., Yousefi A.A. (2003) FTIR studies of  $\beta$ -phase crystal formation in stretched PVDF films, *Polym. Test.* **22**, 6, 699–704.
- Nallasamy P., Mohan S. (2005) Vibrational spectroscopic characterization of form II poly(vinylidene fluoride), *Indian J. Pure Appl. Phys.* **43**, November, 821–827.
- Boccaccio T., Bottino A., Capannelli G., Piaggio P. (2002) Characterization of PVDF membranes by vibrational spectroscopy, *J Membr. Sci.* **210**, 2, 315–329.
- Gomes J., Serrado Nunes J., Sencadas V., Lanceros-Mendez S. (2010) Influence of the  $\beta$ -phase content and degree of crystallinity on the piezo- and ferroelectric properties of poly(vinylidene fluoride), *Smart Mater. Struct.* **19**, 6, 65010.
- Tao M., Liu F., Ma B., Xue L. (2013) Effect of solvent power on PVDF membrane polymorphism during phase inversion, *Desalination* **316**, November, 137–145.

- 23 Peng Y., Sun B., Wu P. (2008) Two-dimensional correlation infrared spectroscopic study on the crystallization and gelation of poly(vinylidene fluoride) in cyclohexanone, *Appl. Spectrosc.* **62**, 3, 295–301.
- 24 Peng Y., Wu P. (2004) A two dimensional infrared correlation spectroscopic study on the structure changes of PVDF during the melting process. *Polym.*, **45**, 15, 5295–5299.
- 25 Lanceros-Méndez S., Mano J.F., Costa A.M., Schmidt V.H. (2001) FTIR and DSC studies of mechanically deformed B-Pvdf films, *J. Macro. Sci. Part B* **40**, 3, 517–527.
- 26 Mohammadi B., Yousefi A.A., Bellah S.M. (2007) Effect of tensile strain rate and elongation on crystalline structure and piezoelectric properties of PVDF thin films, *Polym. Test* **26**, 1, 42–50.
- 27 Sharma M., Madras G., Bose S. (2014) Process induced electroactive  $\beta$ -polymorph in PVDF: effect on dielectric and ferroelectric properties, *Phys. Chem. Chem. Phys.* **16**, 28, 14792–9.
- 28 Cai X., Lei T., Sun D., Lin L. (2017) A critical analysis of the  $\alpha$ ,  $\beta$  and  $\gamma$  phases in poly(vinylidene fluoride) using FTIR, *RSC Adv.* **7**, 25, 15382–15389.
- 29 Bormashenko Y., Pogreb R., Stanevsky O., Bormashenko E. (2004) Vibrational spectrum of PVDF and its interpretation, *Polym. Test* **23**, 7, 791–796.
- 30 Gregorio R. (2006) Determination of the  $\alpha$ ,  $\beta$ , and  $\gamma$  crystalline phases of poly(vinylidene fluoride) films prepared at different conditions, *J. Appl. Polym. Sci.* **100**, 4, 3272–3279.
- 31 Rangel E.Q. (2016) Systematic investigation of the electromechanical properties of Polyvinylidene Fluoride (PVDF) components applied in risers, *Undergraduate Project*, Department of Mechanical Engineering, Pontifical Catholic University of Rio de Janeiro.
- 32 Leo D.J. (2007) *Engineering analysis of smart material systems*, John Wiley & Sons, Inc., Hoboken, NJ.